Angle-dependent magnetoresistance oscillations due to magnetic breakdown orbits

A. F. Bangura,[1,2] P. A. Goddard,[1] J. Singleton,[3] S. W. Tozer,[4] A. I. Coldea,[1,2] A. Ardavan,[1] R. D. McDonald,[3] S. J. Blundell,[1] and J. A. Schlueter[5]

[1]*Clarendon Laboratory, University of Oxford, Parks Road, Oxford OX1 3PU, United Kingdom*

[2]*H. H. Wills Physics Laboratory, University of Bristol, Tyndall Avenue, BS8 1TL, United Kingdom*

[3]*National High Magnetic Field Laboratory, Los Alamos National Laboratory, TA-35, MS-E536, Los Alamos, New Mexico 87545, USA*

[4]*National High Magnetic Field Laboratory, Tallahassee, Florida 83810, USA*

[5]*Materials Science Division, Argonne National Laboratory, Argonne, Illinois 60439, USA*

(Received 17 July 2007; published 23 August 2007)

We present experimental evidence for a hitherto unconfirmed type of angle-dependent magnetoresistance oscillation caused by magnetic breakdown. The effect was observed in the organic superconductor κ-(BEDT-TTF)$_2$Cu(NCS)$_2$ using hydrostatic pressures of up to 9.8 kbar and magnetic fields of up to 33 T. In addition, we show that similar oscillations are revealed in ambient-pressure measurements, provided that the Shubnikov–de Haas oscillations are suppressed either by elevated temperatures or filtering of the data. These results provide a compelling validation of Pippard's semiclassical picture of magnetic breakdown [Philos. Trans. R. Soc. London, Ser. A **270**, 1 (1962)].

DOI: 10.1103/PhysRevB.76.052510 PACS number(s): 74.25.Jb, 71.18.+y, 71.20.Rv, 72.15.Gd

Recently, the measurement of angle-dependent magnetoresistance oscillations (AMROs) has emerged as a powerful technique in the elucidation of the fine details of Fermi surfaces in reduced-dimensionality metals.[1–3] In contrast to de Haas–van Alphen oscillations, AMROs can be observed in rather low-quality samples,[4,5] or when temperatures are relatively high;[6] they have therefore been measured in a wide variety of systems, including crystalline organic metals,[1,7] ruthenates,[2] semiconductor superlattices,[3] and cuprate superconductors.[4] AMROs can, in most cases,[5] be attributed to the time evolution of the quasiparticle velocities as they traverse the Fermi surface under the influence of the magnetic field. Consequently, and based on the topologies of the orbits involved, several distinct species of AMRO have been identified, including Lebed[8,9] and Danner-Chaikin-Kang (DCK) oscillations[10] due to orbits on quasi-one-dimensional (Q1D) sections of Fermi surface, and Yamaji oscillations,[11–13] associated with closed orbits on quasi-two-dimensional (Q2D) Fermi-surface sections (for a detailed description of the differences between these effects, see Ref. 1). In this Brief Report, we report the measurement of a further class of AMROs, observed only at high magnetic fields and caused by magnetic breakdown.

The crystalline organic metal κ-(BEDT-TTF)$_2$Cu(NCS)$_2$ was chosen for the experiments because its Fermi surface both resembles the coupled network model for magnetic breakdown first proposed by Pippard[14] and is very well characterized by theory[15] and experiment.[6,16–18] The Fermi surface is shown in Fig. 1; it comprises a Q2D pocket and a pair of Q1D sheets. The Q2D and Q1D sections are separated in k space at the Brillouin-zone boundary owing to a weak periodic potential caused by the translational symmetry of the anion layers.[7] At sufficiently high magnetic fields B, mixing between the states on the two Fermi-surface sections leads to magnetic breakdown, in which a quasiparticle "tunnels" in k space between them.[14,17,19] In Pippard's semiclassical picture,[14] this enables quasiparticles to execute the large β orbit (Fig. 1) and other more complex orbits about the Fermi surface, leading to the observation of high-frequency Shubnikov–de Haas (SdH) and de Haas–van Alphen oscillations.[17,20,21] The probability

$$P = \exp(-B_0/B) \tag{1}$$

of magnetic breakdown is parametrized by B_0, the characteristic *breakdown field*.[14,17,19] In this Brief Report, we show that magnetic breakdown can additionally produce a different type of AMRO in κ-(BEDT-TTF)$_2$Cu(NCS)$_2$. The origin of this phenomenon is similar to that of Yamaji oscillations[6] but in the present case, the quasiparticle trajectories responsible are *magnetic breakdown orbits*, rather than closed paths on Q2D Fermi-surface sections. In order to distinguish the new features from the more conventional Lebed or Yamaji oscillations, we will refer to them as breakdown AMROs or BAMROs.

Four-wire magnetotransport experiments are performed on single crystals of κ-(BEDT-TTF)$_2$Cu(NCS)$_2$ in quasistatic fields produced by 33 T Bitter coils and the 45 T hybrid magnet at NHMFL Tallahassee. A two-axis goniometer allows continuous rotation of the angle θ between the applied magnetic field and the normal to the highly conductive planes of the sample, as well as discrete changes in the plane of rotation parametrized by the azimuthal angle ϕ. [In κ-(BEDT-TTF)$_2$Cu(NCS)$_2$, we define the ϕ=0° plane of rotation as being perpendicular to the Q1D sheets.] The goniometer is placed within a ^{3}He cryostat allowing temperatures T as low as 500 mK. Electrical contacts are applied to the samples using 12.5 μm Au or Pt wires attached using graphite paint. For the high-pressure measurements, the samples are placed inside a miniature anvil cell of length 9 mm and outer diameter 6 mm.[22] Pressure (p) measurement is performed *in situ* using the ruby fluorescence line at ≈690 nm, excited using the 448 nm line of an Ar-ion laser; the pressure dependence of this ruby line is well known.[23] A single optical fiber is used to excite and collect the fluorescence of a chip of ruby placed within the cell next to the sample, and is compared to that of a chip at the same T outside the pressure cell. Typical κ-(BEDT-TTF)$_2$Cu(NCS)$_2$ sample dimensions

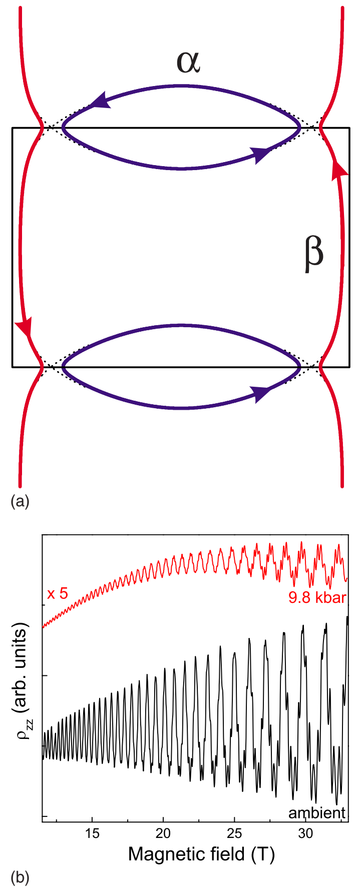

FIG. 1. (Color online) (a) In plane Fermi-surface of κ-(BEDT-TTF)$_2$Cu(NCS)$_2$, showing the closed Q2D pockets (blue), the open Q1D sheets (red), and the Brillouin zone boundary (black). The dotted lines show the possible semiclassical paths between the Q1D and Q2D Fermi-surface sections at the zone boundary taken by a quasiparticle on the breakdown β orbit. (b) Shubnikov–de Haas oscillations observed in two κ-(BEDT-TTF)$_2$Cu(NCS)$_2$ samples at $T\sim 500$ mK, with the magnetic field directed perpendicular to the conducting planes ($\theta=0°$). The upper trace is for a sample at a pressure $p=9.8\pm0.2$ kbar; the other is at ambient pressure. At low fields a single oscillation frequency is present corresponding to the α orbit. At larger fields, higher frequencies are seen, corresponding to the β orbit and other magnetic breakdown orbits (Ref. 17). The 9.8 kbar data are enhanced by a factor of 5 and the curves are offset for clarity.

are $\sim 0.7\times0.5\times0.1$ mm^3 for the ambient-pressure experiments and $\sim 0.1\times0.1\times0.04$ mm^3 for the high-pressure measurements.

Data such as those in Fig. 1 were Fourier analyzed to reveal the SdH oscillation frequencies F present. In addition to frequencies due to the classically allowed α orbit about the Q2D pocket (F_α) and the β breakdown orbit (F_β), combination frequencies such as $F_\beta - F_\alpha$ and $F_\beta - 2F_\alpha$ caused by the Shiba-Fukuyama-Stark quantum interference effect[7,17,20,21] are observed in the Fourier transforms. The frequencies found were $F_\alpha=750\pm20$ T and $F_\beta=4030\pm60$ T at $p=9.8$ kbar and $F_\alpha=610\pm10$ T and $F_\beta=3950\pm30$ T at ambient pressure. In addition, the B and T dependences of the F_α frequency Fourier amplitudes were fitted using the standard Lifshitz-Kosevich formalism appropriate for a 2D metal.[17,19] In this way the effective mass m_α^* at $\theta=0°$ and "Dingle" scattering time τ_α (Refs. 19 and 24) of the α-pocket quasiparticles at 9.8 kbar were determined to be 2.0 ± 0.1 m_e and 0.81 ± 0.05 ps, respectively, where m_e is the electron rest mass; equivalent values for the ambient-pressure experiments were 3.5 ± 0.1 m_e and 2.3 ± 0.2 ps. These masses and frequencies are in reasonable agreement with previous high-pressure SdH data.[18]

An earlier study of AMROs in ambient-pressure κ-(BEDT-TTF)$_2$Cu(NCS)$_2$ (Ref. 6) found that the magnetoresistance features for angles $\theta\gtrsim 70°$ may be attributed to Lebed, Yamaji, or DCK oscillations, depending on the azimuthal angle ϕ. It was also found that the Lebed and Yamaji oscillations do not tend to coexist at the same ϕ.[6] The Lebed oscillations dominate when the plane of rotation of the field is roughly perpendicular to the Q1D sheets ($\phi\approx 0°$); the Yamaji oscillations are more prominent when the plane of rotation of the field is close to that containing the short axis of the Q2D α pocket ($\phi\approx 90°$).[6] Applying the same analysis[6] to the $p=9.8$ kbar AMRO data in this Brief Report, the ϕ angles at which the Lebed or Yamaji oscillations dominate are found to be comparable to those at ambient pressure.

However, an additional series of AMROs is observed for *all* ϕ when $\theta\lesssim 70°$. Like the Yamaji and Lebed oscillations, the extra series is periodic in tan θ, but its frequency is considerably higher. To illustrate this, Fig. 2(a) shows AMRO data at $p=9.8$ kbar. Two sets of oscillations are clearly seen, both periodic in tan θ. The frequencies of the features appearing at tan $\theta\gtrsim 3$ show them to be the Lebed oscillations expected for this value of ϕ.[6] The faster oscillations are only observed at tan $\theta\lesssim 3$ ($\theta\lesssim 70°$); it is these oscillations that we will identify below as BAMROs. The fact that the latter oscillations are observed with a similar frequency at all planes of rotation suggests that they result from a rather isotropic, Q2D quasiparticle orbit.

Given such an orbit, the tan θ frequency of the resulting AMROs at a given ϕ angle should be proportional to $k_\parallel^{\max}$, the maximum in-plane wave vector of the orbit projected onto the plane of rotation of the field.[25] For oscillations arising from an elliptical cross-section orbit, $k_\parallel^{\max}(\phi)$ can be fitted to the equation

$$k_\parallel^{\max}(\phi) = [k_a^2\cos^2(\phi-\zeta) + k_b^2\sin^2(\phi-\zeta)]^{1/2}, \qquad (2)$$

where k_a and k_b are the major and minor semiaxes of the ellipse, respectively, and ζ is the angle between its major axis and the $\phi=0°$ direction.[25]

The $k_\parallel^{\max}(\phi)$ values for the higher-frequency AMROs (tan $\theta\lesssim 3$) at 9.8 kbar are plotted in Fig. 2(b) (red circles). An unconstrained fit to Eq. (2) implies that the orbit that gives rise to the oscillations is almost circular in cross section with an area $(3.8\pm0.1)\times10^{19}$ m^{-2}. Within the experimental errors, this value agrees with the area of the β orbit determined from the SdH frequency $[(3.84\pm0.05)\times10^{19}$ m$^{-2}]$ measured at 9.8 kbar. The good agreement strongly suggests that the high-frequency AMROs are BAMROs caused by β orbits that completely traverse the

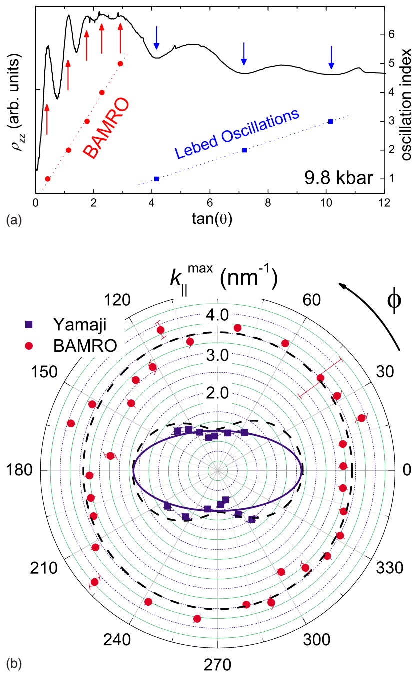

FIG. 2. (Color online) (a) Magnetoresistance of κ-(BEDT-TTF)$_2$Cu(NCS)$_2$ (black curve) as a function of tan θ at p=9.8 kbar, B=30 T, T=1.5 K, and ϕ=160°. The positions of the BAMROs are marked with up (red) arrows and the Lebed oscillations with down (blue) arrows. Also shown are these positions as a function of oscillation index (points) from which the frequencies may be extracted. (b) Polar plot of the maximum in-plane Fermi wave vector, $k_{\parallel}^{\max}$, derived from the tan θ oscillation frequency, as a function of ϕ. Blue squares are Yamaji oscillations and red circles are BAMROs. Fits of Eq. (2) to the data (dashed lines) allow the geometry of the orbits which give rise to the oscillations to be determined. The dimensions of the α orbit thus derived are shown (blue solid line). The error in ϕ is ±5°.

Q1D and Q2D Fermi-surface sections; i.e., they are only made possible by magnetic breakdown.

For comparison, Fig. 2(b) also presents the values of $k_{\parallel}^{\max}$ determined from the Yamaji oscillations due to the α pocket (tending to occur at tan $\theta \gtrsim 3$).[6] These data (blue squares) are plotted against ϕ for all planes of rotation at which they are observed; at the others the Lebed oscillations dominate.[6] The dashed line is a fit to Eq. (2), where the area is constrained by F_α from the SdH data. The semimajor and semiminor axes of the α pocket obtained in this manner are 2.2±0.2 and 1.06±0.09 nm^{-1}, respectively. Therefore, in good quantitative agreement with earlier work,[18,27] we find that the effect of increased pressure is to make the α pocket less elongated.

Increased hydrostatic pressure is known to reduce the breakdown field B_0 in κ-(BEDT-TTF)$_2$Cu(NCS)$_2$,[18] enhancing the likelihood of magnetic breakdown [see Eq. (1)]. Having identified BAMROs at p=9.8 kbar, it is instructive to see if the same effect occurs at ambient pressure where the breakdown probability is lower. Figure 3(a) shows the angle-dependent magnetoresistance measured at ambient pressure, B=42 T, T=1.5 K, and ϕ=160°. The upper curve comprises raw data; as in Fig. 2, Lebed oscillations are seen at tan $\theta \gtrsim 3$. However, at lower values of tan θ, the data are dominated by SdH oscillations from the α orbit.[6] The lower curve in Fig. 3(a) shows the same data after numerical processing to remove the SdH oscillations (the abscissa is converted to B cos θ and the data passed through a low-pass Fourier transform filter with a 100 T cut-off frequency). The filtering reveals the presence of AMROs, previously hidden by the SdH, that are periodic in tan θ and almost identical to the BAMROs seen at 9.8 kbar. A fit to Eq. (2) of the ϕ dependence of the frequency of these oscillations gives an orbit area of $(3.4\pm0.3)\times 10^{19}$ m^{-2}, in reasonable agreement with that obtained from F_β in the ambient-pressure SdH data $[(3.76\pm0.03)\times 10^{19}$ m$^{-2}]$.

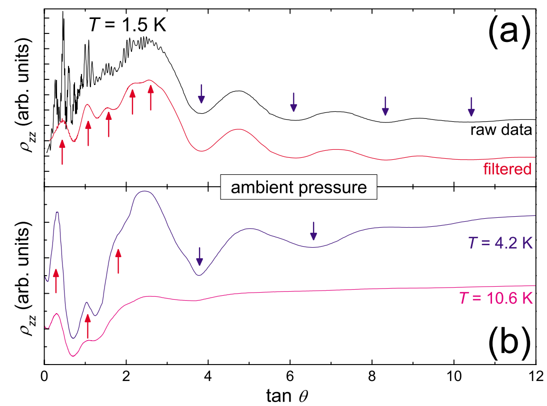

FIG. 3. (Color online) Ambient-pressure angle-dependent magnetoresistance. (a) Comparison of data taken at B=42 T, T=1.5 K, and ϕ=160° before (upper curve) and after (lower curve) filtering to remove the SdH oscillations. (b) Data taken at a similar ϕ angle with B=45 T. Two temperatures are shown, T=4.2 K (upper curve) and T=10.6 K. In both (a) and (b), up (red) arrows mark the BAMROs, down (blue) arrows mark the Lebed oscillations, and the curves are offset for clarity.

Figure 3(b) shows data taken at a ϕ similar to that in (a) but at higher T. AMROs are known to be robust at lower B/T than magnetic quantum oscillations as they do not depend so strongly on thermal smearing of the Fermi surface.[5,26] Thus, at T=4.2 K the SdH oscillation are no longer visible, whereas both the BAMROs and Lebed oscillations are clearly observed. Indeed, both are still discernible at T =10.6 K, albeit with a reduced amplitude.[26]

Thus, it appears that BAMROs are observable in κ-(BEDT-TTF)$_2$Cu(NCS)$_2$ at ambient pressure. A comparison with Fig. 2(a), in which the BAMROs appear to be more prominent compared to the background than the features seen in the filtered data of Fig. 3(a), measured at the same temperature but at a higher magnetic field, indeed suggests that the enhanced breakdown probability at higher pressures promotes the BAMRO mechanism. However, a more significant factor in explaining why the BAMROs are so clear in the high-pressure data, but somewhat concealed in ambient-pressure data, is the relative strength of the SdH oscillations. The sample used in the pressure studies exhibits a significantly lower Dingle scattering time ($\tau_\alpha \approx 0.81$ ps) than the sample used for the ambient-pressure experiments (τ_α ≈ 2.3 ps). Even though m_α decreases from 3.5 m_e to 2.0 m_e on going from ambient pressure to 9.8 kbar (see above and

Ref. 18), the Dingle scattering time is reduced by a greater factor, greatly suppressing the SdH oscillations in the 9.8 kbar experiments.

Elevated T's also suppress SdH oscillations[26] [Fig. 3(b)], revealing the underlying BAMROs. The fact the BAMRO features survive at scattering times and T's at which the SdH cannot be observed is further evidence that their mechanism is related to semiclassical quasiparticle trajectories across the Fermi surface, similar to those invoked to explain Yamaji oscillations.[6,26]

Therefore, we believe that, although present, BAMROs have not previously been identified in κ-(BEDT-TTF)$_2$Cu(NCS)$_2$ because, in general, angle-dependent magnetotransport measurements are performed at low T's with the cleanest possible samples.[6] Under these conditions, the data at the θ angles where BAMROs are observed are dominated by the SdH oscillations.

All AMROs are progressively damped as θ increases. In κ-(BEDT-TTF)$_2$Cu(NCS)$_2$, this is known to occur because the amplitude of the Yamaji and Lebed oscillations is governed by the value of $\omega\tau$, where ω is an angular frequency of the orbit responsible and τ is a scattering time.[26] The orbit frequency depends on the projection of the magnetic field, and so $\omega \propto \cos\theta$, leading to a decrease in $\omega\tau$ and hence AMRO amplitude as θ increases.[26] However, compared to conventional AMROs, BAMROs will have an additional damping factor due to Eq. (1), because in Q2D systems such as κ-(BEDT-TTF)$_2$Cu(NCS)$_2$, B_0 is found to be inversely proportional to $\cos\theta$.[17,19] The factor of $\cos\theta$ leads to additional attenuation as θ increases, so that the BAMROs are only noticeable for $\theta \lesssim 70°$.

In summary, we have shown conclusive experimental evidence of BAMROs, angle-dependent magnetoresistance oscillations caused by magnetic breakdown. Magnetic breakdown has been interpreted semiclassically in terms of quasiparticle orbits that jump gaps between Fermi surfaces in k space.[14] This model has been extensively explored via a detailed analysis of the magnetoresistance oscillations that arise in Mg due to the quantum interference of the quasiparticle orbits (see Ref. 28 and references therein). The observation of BAMROs provides a further compelling validation of this picture of magnetic breakdown, and in addition represents the only experimental manifestation of magnetic breakdown that can be described in purely semiclassical terms.

This work is funded by U.S. Department of Energy (DOE) LDRD Grants Nos. 20040326ER, 20030084DR, and 20070013DR and by EPSRC Grant No. GR/T27341/01 (U.K.). NHMFL is supported by the NSF, DOE, and the State of Florida. Work at Argonne was supported by the Office of Basic Energy Sciences, U.S. DOE (Contract No. W-31-109-ENG-38). A.A. and A.I.C. acknowledge support from the Royal Society and PAG from the Oxford University Glasstone Fund.

[1] M. V. Kartsovnik, Chem. Rev. (Washington, D.C.) **104**, 5737 (2004).
[2] E. Ohmichi, Y. Maeno, and T. Ishiguro, J. Phys. Soc. Jpn. **68**, 24 (1999).
[3] M. Kawamura, A. Endo, M. Hirasawa, S. Katsumoto, and Y. Iye, Physica B **249-251**, 882 (1998).
[4] N. E. Hussey, M. Abdel-Jawad, A. Carrington, A. P. Mackenzie, and L. Balicas, Nature (London) **425**, 814 (2003).
[5] S. J. Blundell and J. Singleton, Phys. Rev. B **53**, 5609 (1996).
[6] P. A. Goddard, S. J. Blundell, J. Singleton, R. D. McDonald, A. Ardavan, A. Narduzzo, J. A. Schlueter, A. M. Kini, and T. Sasaki, Phys. Rev. B **69**, 174509 (2004).
[7] J. Singleton, Rep. Prog. Phys. **63**, 1111 (2000).
[8] A. G. Lebed and P. Bak, Phys. Rev. Lett. **63**, 1315 (1989).
[9] Lebed's explanation of AMROs was derived for Q1D TMTSF salts and involves the quasiparticles undergoing a dimensionality crossover at certain *magic angles*. It was later shown that similar features in other materials [including κ-(BEDT-TTF)$_2$Cu(NCS)$_2$] can be accounted for semiclassically via the Boltzmann transport equation (Ref. 5).
[10] G. M. Danner, W. Kang, and P. M. Chaikin, Phys. Rev. Lett. **72**, 3714 (1994).
[11] M. V. Kartsovnik, P. A. Kononovich, V. N. Laukhin, and I. F. Shchegolev, JETP Lett. **48**, 541 (1988).
[12] K. Yamaji, J. Phys. Soc. Jpn. **58**, 1520 (1989).
[13] R. Yagi, Y. Iye, T. Osada, and S. Kagoshima, Synth. Met. **42**, 2237 (1991).
[14] A. B. Pippard, Philos. Trans. R. Soc. London, Ser. A **270**, 1 (1962).
[15] K. Oshima, T. Mori, H. Inokuchi, H. Urayama, H. Yamochi, and G. Saito, Phys. Rev. B **38**, 938 (1988).
[16] N. Toyota, E. W. Fenton, T. Sasaki, and M. Tachiki, Solid State Commun. **72**, 859 (1989).
[17] N. Harrison, J. Caulfield, J. Singleton, P. H. P. Reinders, F. Herlach, W. Hayes, M. Kurmoo, and P. Day, J. Phys.: Condens. Matter **8**, 5415 (1996).
[18] J. Caulfield, W. Lubczynski, F. L. Pratt, J. Singleton, D. Y. K. Ko, W. Hayes, M. Kurmoo, and P. Day, J. Phys.: Condens. Matter **6**, 2911 (1994).
[19] D. Shoenberg, *Magnetic Oscillations in Metals* (Cambridge University Press, Cambridge, 1984).
[20] M. V. Kartsovnik, G. Yu. Logvenov, T. Ishiguro, W. Biberacher, H. Anzai, and N. D. Kushch, Phys. Rev. Lett. **77**, 2530 (1996).
[21] I. Mihut, C. C. Agosta, C. Martin, C. H. Mielke, T. Coffey, M. Tokumoto, M. Kurmoo, J. A. Schlueter, P. Goddard, and N. Harrison, Phys. Rev. B **73**, 125118 (2006).
[22] S. W. Tozer, Rev. Sci. Instrum. **64**, 2607 (1993).
[23] J. D. Barnett, S. Block, and G. J. Piermarini, Rev. Sci. Instrum. **44**, 1 (1973).
[24] J. Singleton, in *Encyclopedia of Condensed Matter Physics*, edited by G. Bassani, G. Liedl, and P. Wyder (Elsevier, Oxford, 2005), p. 343.
[25] A. A. House, N. Harrison, S. J. Blundell, I. Deckers, J. Singleton, F. Herlach, W. Hayes, J. A. A. J. Perenboom, M. Kurmoo, and P. Day, Phys. Rev. B **53**, 9127 (1996).
[26] J. Singleton, P. A. Goddard, A. Ardavan, A. I. Coldea, S. J. Blundell, R. D. McDonald, S. Tozer, and J. A. Schlueter, Phys. Rev. Lett. **99**, 027004 (2007).
[27] T. Biggs, A.-K. Klehe, J. Singleton, D. Bakker, J. Symington, P. Goddard, A. Ardavan, W. Hayes, J. A. Schlueter, T. Sasaki, and M. Kurmoo, J. Phys.: Condens. Matter **14**, L495 (2002).
[28] R. Reifenberger, J. Low Temp. Phys. **26**, 827 (1977).